

Equilibrium and Kinetic Study of Interaction of Amino Acid Inhibitors with Tryptophanase: Mechanism of Quinonoid Formation[†]

David S. June,[‡] Clarence H. Suelter,* and James L. Dye

ABSTRACT: Tryptophanase, a pyridoxal phosphate dependent enzyme, with pH-dependent absorption maxima at 337 and 420 nm due to bound pyridoxal phosphate, interacts with several amino acid inhibitors to form stable, dead-end quinonoid complexes characterized by an intense absorption band centered around 500 nm [Watanabe, T., & Snell, E. E. (1977) *J. Biochem. (Tokyo)* 82, 733-745]. Stopped-flow studies of the kinetics of formation of the quinonoid with the inhibitor, ethionine, showed that the 420-nm form of the enzyme is the active form. This assignment is supported by the following observations: (1) the rate constant for disappearance of the 420-nm absorbance ($18.0 \pm 2.2 \text{ s}^{-1}$) was the same as that of the fast phase of the biphasic growth of quinonoid at 508 nm ($15.0 \pm 1.2 \text{ s}^{-1}$) (listed uncertainties are marginal standard deviation estimates based upon a least-squares analysis of the data according to the selected model); (2) the rate of disappearance of the 337-nm absorbance is the same as the rate of the slow phase of quinonoid formation and is essentially unaffected by the inhibitor concentration or the nature of the inhibitor, ethionine or alanine; (3) the average rate constant for the slow phase obtained with ethionine, $0.51 \pm 0.14 \text{ s}^{-1}$,

agrees closely with the rate constant for the conversion of the 337-nm form, conformation γ , to the 420-nm form, conformation β , following a rapid decrease in pH [June, D. S., Suelter, C. H., & Dye, J. L. (1981) *Biochemistry* (preceding paper in this issue)]. Thus the 337-nm form apparently does not form quinonoid directly but is first converted to the 420-nm form before the α proton of an amino acid inhibitor is removed to form quinonoid. The kinetics of biphasic quinonoid formation, the amplitudes of the slow and fast phases, the pH dependence of the rate of interconversion of the various forms of tryptophanase, and the equilibrium data for the formation of quinonoid as a function of pH are all consistent with this scheme. Comparison of the kinetics of formation of quinonoid with L-[α -¹H]alanine and L-[α -²H]alanine showed a deuterium isotope effect of 4.9 on the rate constant and 4.5 on the equilibrium constant for quinonoid formation. This shows that the rate-limiting step of quinonoid formation is the abstraction of the α proton. The rate constant for this step with ethionine (protio) is $25.7 \pm 1.5 \text{ s}^{-1}$, and the extinction coefficient at 508 nm for the quinonoid with ethionine is $(4.04 \pm 0.05) \times 10^4 \text{ M}^{-1} \text{ cm}^{-1}$.

Tryptophanase (EC 4.1.99.1), a pyridoxal-P¹ enzyme which requires monovalent cations for optimum catalytic activity, has pH-dependent absorption maxima at 337 and 420 nm due to bound pyridoxal-P (Morino & Snell, 1967). When tryptophanase interacts with a competitive inhibitor such as alanine, a stable, dead-end quinonoid complex, characterized by an intense absorption centered at 502 nm, is produced (Morino & Snell, 1967). Recently several additional inhibitors, including ethionine, that form quinonoid derivatives with tryptophanase have been identified (Watanabe & Snell, 1977). The kinetics of the interconversion of the 337- and 420-nm forms following a rapid change in pH was described in a preceding paper (June et al., 1981) by a scheme involving three conformations with different absorption maxima: β , $\lambda_{\text{max}} = 420 \text{ nm}$; γ , $\lambda_{\text{max}} = 337 \text{ nm}$; δ , $\lambda_{\text{max}} = 355 \text{ nm}$.

This paper describes a kinetic study of the changes in absorbance at 420, 337, and 508 nm following the interaction with ethionine, a study of the equilibrium reaction between ethionine and tryptophanase as a function of pH, and the effect of deuterium substitution at the α position of alanine. The results support and extend the scheme previously used to describe the pH- and time-dependent interconversion of the 337- and 420-nm spectral forms of tryptophanase (June et al., 1981). A study of the catalytic events following the interaction with substrates will be described at a later date.

Materials and Methods

Reagents. Pyridoxal 5'-phosphate and *N*-(2-hydroxyethyl)piperazinepropanesulfonic acid (Hepps) were obtained from Sigma Chemical Co. $(\text{CH}_3)_4\text{NCl}$ from Aldrich Chemical Co. was recrystallized from 1-propanol before use. $(\text{CH}_3)_4\text{NOH}$ was prepared fresh before use by passage of recrystallized $(\text{CH}_3)_4\text{NCl}$ over Dowex 1-OH. L-Ethionine was from Vega Biochemicals, Tucson, AZ, and L-[α -²H]alanine was purchased from Merck and Co. Inc., Rahway, NJ.

Tryptophanase. Tryptophanase from *Escherichia coli* B/1t7-A was prepared as described by Watanabe & Snell (1972) including the modification of Suelter et al. (1977). Protein was judged to be >95% tryptophanase by polyacrylamide gel electrophoresis. Holoenzyme was prepared from stock apoenzyme by incubation in 0.1 M potassium phosphate, pH 8.0, 7% $(\text{NH}_4)_2\text{SO}_4$, 1 mM EDTA, 0.2 mM pyridoxal-P, and 20 mM dithiothreitol (DTT) for 1 h at 37 °C. Occasionally, activation was achieved in the same buffer at 50 °C for 15 min as suggested by Hogberg-Raubaud et al. (1975). The enzyme had a specific activity of 40–55 $\mu\text{mol min}^{-1} \text{ mg}^{-1}$ when assayed with 0.6 mM S-(*o*-nitrophenyl)-L-cysteine (SOPC) in 50 mM potassium phosphate, pH 8.0, and 50 mM KCl, at 30 °C (Suelter et al., 1976). Protein concentration was determined spectrophotometrically by using $\epsilon_{278} = 0.795 \text{ mL mg}^{-1} \text{ cm}^{-1}$ (Morino & Snell, 1967).

Scanning Stopped-Flow Experiments. These experiments were completed with a computerized double-beam rapid-

[†] From the Department of Biochemistry (C.H.S.) and the Department of Chemistry (J.L.D.), Michigan State University, East Lansing, Michigan 48824. Received April 28, 1980; revised manuscript received October 15, 1980. This work was supported by National Science Foundation Grant PCM 78-15750.

[‡] Present address: Marion Laboratories, Kansas City, MO 64137.

¹ Abbreviations used: DTT, DL-dithiothreitol; Hepps, *N*-(2-hydroxyethyl)piperazinepropanesulfonic acid; EDTA, ethylenediaminetetraacetic acid; SOPC, S-(*o*-nitrophenyl)-L-cysteine; pyridoxal-P, pyridoxal 5'-phosphate.

scanning stopped-flow instrument described elsewhere (Coolen et al., 1975; Papadakis et al., 1975) at $24.0 \pm 0.3^\circ\text{C}$ with a 1.85-cm path length. Scanning data as well as fixed wavelength data were collected by using an averaging scheme previously described (Suelter et al., 1975). A scanning time of 6.7 ms over the wavelength range 280–600 nm was used. Control spectra were collected as outlined previously (June et al., 1979). Experimental conditions for individual experiments are described below.

Kinetics of Interaction of Tryptophanase with Ethionine. Activated holotryptophanase (10 mg mL^{-1}) was equilibrated by dialysis at 4°C with 25 mM K-Hepps, pH 8.0, 0.1 M KCl, 1 mM EDTA, 0.1 mM pyridoxal-P, and 0.2 mM DTT and diluted to a concentration of 1.4 mg mL^{-1} with the same buffer (sp act. = $51\text{ }\mu\text{mol min}^{-1}\text{ mg}^{-1}$). This enzyme solution was pushed against various concentrations of L-ethionine in 25 mM K-Hepps, pH 8.0, and 0.1 M KCl.

For the data presented in Figure 1, holotryptophanase was equilibrated with 25 mM K-Hepps, pH 8.0, 0.2 M KCl, 1 mM EDTA, 10 μM pyridoxal-P, and 0.2 mM DTT and then diluted to a concentration of 1.3 mg mL^{-1} (sp act. = $40\text{ }\mu\text{mol min}^{-1}\text{ mg}^{-1}$) before being pushed against 20 mM L-ethionine in the same buffer. For the study at three pH values (Table III) activated holotryptophanase (20 mg mL^{-1}) was equilibrated by dialysis at 4°C with 25 mM K-Hepps, pH 8.0, 0.1 M KCl, 1 mM EDTA, 0.1 mM pyridoxal-P, and 0.2 mM DTT. The enzyme was divided into three equal volumes at a concentration of 1.6 mg mL^{-1} (sp act. = $51\text{ }\mu\text{mol min}^{-1}\text{ mg}^{-1}$). These three solutions were adjusted to pH values of 7.2, 8.0, and 8.7, with 0.1 M HCl or 0.1 M KOH at 24°C and pushed against 25 mM K-Hepps, 0.1 M KCl, and 10 mM L-ethionine at pH 7.2, 8.0, or 8.7.

Kinetics of Interaction of Tryptophanase with L-[α -H]-Alanine and L-[α - ^2H]Alanine. Activated holotryptophanase (20 mg mL^{-1}) was equilibrated by dialysis at 4°C with 25 mM K-Hepps, pH 8.0, 0.1 M KCl, 1 mM EDTA, 0.1 mM pyridoxal-P, and 0.2 mM DTT and diluted to a concentration of 1.8 mg mL^{-1} (sp act. = $51\text{ }\mu\text{mol min}^{-1}\text{ mg}^{-1}$). This enzyme solution was pushed against 25 mM K-Hepps, pH 8.0, 0.1 M KCl, 1 mM EDTA, and 0.1 mM pyridoxal-P containing 0.45 M L-[α - ^1H]alanine or L-[α - ^2H]alanine.

pH Dependence of Equilibrium Concentrations of Tryptophanase and Ethionine. One-tenth milliliter of tryptophanase ($\sim 25\text{ mg mL}^{-1}$, sp act. = $48\text{ }\mu\text{mol min}^{-1}\text{ mg}^{-1}$) in 1 mM imidazole-HCl, pH 8.0, 0.2 M KCl, 0.1 mM pyridoxal-P, 1 mM EDTA, and 10 mM β -mercaptoethanol was added to 0.9 mL of 0.025 M imidazole-HCl, pH_i, 0.2 M KCl, 1 mM EDTA, and 0.1 mM pyridoxal-P in a quartz cuvette. Aliquots of 0.16 M ethionine in 0.1 mM pyridoxal-P, 0.2 M KCl, and 1 mM EDTA at pH_f were added to a cuvette, and the absorbance was measured at 508 nm. The final pH of each titration was measured after addition of the last aliquot of ethionine.

Data Analysis. Data were fitted by the appropriate mathematical function using the nonlinear curve-fitting program KINFIT4 (Dye & Nicely, 1971). Errors listed are marginal standard deviations and therefore include the effects of coupling among the parameters.²

The absorbance, A , for single exponential growth or decay was fitted by eq 1. The three adjustable parameters were A_∞ ,

$$A = A_\infty - \Delta A e^{-k_1' t} \quad (1)$$

the absorbance at infinite time, ΔA , the total change in ab-

Table I: Rate Constants and Amplitudes^a for Absorbance Changes at 337, 420, and 508 nm When Tryptophanase Is Mixed with L-Ethionine As Described in the Legend to Figure 1

wavelength (nm)	k_1' (s^{-1})	k_2' (s^{-1})	total ΔA
508 (growth)	15.0 (1.2) ^b	0.63 (6)	0.747 ^c
420 (decay)	18.0 (2.2)		0.049 (1)
420 (growth) ^d		0.38 (5)	0.017 (1)
337 (growth)		0.56 (8)	0.026 (1)

^a The data at 508 nm were fit with eq 2. The data at 337 nm were fit with eq 1. The data at 420 nm are composed of two parts as described in the text; each part was fit separately with eq 1. ^b Numbers in parentheses are the marginal standard deviation estimates for the last significant figure. ^c 58% fast phase; 42% slow phase. Path length, 1.85 cm. ^d The slow growth of absorbance at 420 nm following the fast phase is due to the nonenzymatic formation of a Schiff base between excess free ethionine and pyridoxal-P as determined in a separate experiment (data not given).

sorbance, i.e., $A_\infty - A_0$ where A_0 equals the absorbance at $t = 0$, and k_1' , the apparent first-order rate constant.

Biphasic data were analyzed as the sum of two exponentials according to eq 2

$$A = A_\infty - \Delta A_1 e^{-k_1' t} + \Delta A_2 e^{-k_2' t} \quad (2)$$

where A_∞ is the measured absorbance at infinite time, ΔA_1 and ΔA_2 are the changes in absorbance due to the fast and slow phases, respectively, and k_1' and k_2' are the apparent first-order rate constants for the fast and slow phases.

Results

Kinetics of Interaction of Ethionine with Tryptophanase. As indicated in the introduction, tryptophanase exhibits absorption bands due to bound coenzyme at 337 and 420 nm, and following interaction with a dead-end inhibitor, such as ethionine, a new absorption appears near 500 nm. The 337-nm form had been previously associated with active enzyme on the basis that at pH values above 8.0, where tryptophanase appeared to exhibit its greatest activity, the 337-nm form predominated (Morino & Snell, 1967). In fact, completely inactive enzyme has an absorbance maximum at 420 nm. In addition, the effective monovalent cation activators promote formation of the 337-nm form. Yet significant amounts of the 420-nm absorbance remain at the apparent pH optimum of 8.3 (June et al., 1981). This and the fact that measurable activity is observed in the presence of LiCl (Suelter & Snell, 1977), when the enzyme shows practically no 337-nm form, prompted us to investigate the spectral forms of tryptophanase in a more quantitative manner in an attempt to determine the roles played by the 337- and 420-nm forms in catalysis. We reasoned that by simultaneously following the changes in absorbance at 337, 420, and 508 nm after mixing tryptophanase with ethionine in a scanning stopped-flow spectrophotometer, we might be able to correlate the rates of change at 337 or 420 nm with the 508-nm absorbance and thus assess the importance of each form to the activity of the enzyme.

Figure 1 shows the changes, summarized in Table I, which occurred in the tryptophanase spectrum at 337, 420, and 508 nm after mixing ethionine with tryptophanase. The 508-nm quinonoid showed a biphasic growth with first-order rate constants of $15 \pm 1.2\text{ s}^{-1}$ and $0.62 \pm 0.06\text{ s}^{-1}$ for the fast and slow phases, respectively (Figure 1A). The loss of the 420-nm band was rapid with a first-order rate constant of $18 \pm 2.2\text{ s}^{-1}$, while the 337-nm form of the coenzyme disappeared slowly with an apparent first-order rate constant of $0.50 \pm 0.08\text{ s}^{-1}$. Therefore, the rapid phase of quinonoid growth occurs simultaneously with the loss of the 420-nm absorbance while

² Standard deviation estimates are used throughout this paper.

Table II: Rate Constants and Amplitudes for Biphasic Growth of Quinonoid at pH 8.00 as a Function of Ethionine and Alanine Concentrations Determined with Scanning Stopped-flow Spectrophotometer in the Fixed-Wavelength Mode^a

inhibitor (mM)	k_1' obsd (s^{-1})	k_1' calcd ^c (s^{-1})	k_2' (s^{-1})	ΔA_1 (%)	total ΔA	$(\Delta A_1)_{\text{obsd}}/(\Delta A_1)_{\text{calcd}}^d$
[L-ethionine]						
0.30	2.26 (2) ^b	2.66	0.377 (4)	70	0.172	0.62
0.40	3.05 (2)	3.00	0.409 (12)	64	0.247	0.70
0.75	4.42 (2)	4.09	0.416 (8)	59	0.340	0.68
1.0	5.20 (8)	4.81	0.418 (1)	56	0.381	0.66
1.5	7.15 (6)	6.13	0.452 (4)	54	0.452	0.68
5.0	14.0 (1)	12.3	0.613 (5)	52	0.562	0.69
10	16.9 (3)	16.7	0.712 (3)	55	0.591	0.74
20	17.5 (5)	20.6	0.717 (17)	57	0.442 ^e	
[L-alanine]						
50	2.24 (6)		0.386 (11)	50		
100	2.21 (12)		0.437 (28)	50		
200	2.74 (12)		0.59 (44)	49		

^a The concentrations of the reaction components after mixing were 25 mM K-Hepps, pH 8.0, 0.1 M KCl, 0.5 mM EDTA, 0.05 mM pyridoxal-P, 0.1 mM DTT, and 0.7 mg mL⁻¹ tryptophanase. Kinetic constants and amplitudes were obtained by fitting the data for the change in absorbance at ~508 nm for ethionine and ~502 nm for alanine as a function of time with eq 2. Percent ΔA_1 is the percentage of the total absorbance change attributable to the first phase. ^b Numbers in parenthesis are the marginal standard deviation estimates for the last significant figure. ^c Calculated with eq 4 by using the best-fit parameters given in Table IV. ^d Calculated by procedures described under Discussion. ^e These data were collected at a somewhat lower wavelength and therefore are not included in the comparison. Path length, 1.85 cm.

the slow phase of quinonoid growth occurs concurrently with the loss of the 337-nm form, showing that a form which absorbs at 420 nm is the one poised for reaction. The observed slow increase at 420 nm following the fast phase is due to the nonenzymatic formation of a Schiff base between excess free ethionine and pyridoxal-P (determined in a separate experiment, data not given).

The next experiments were carried out to define the concentration dependence of the kinetics of interaction of ethionine with tryptophanase. As shown in Figure 1A, the growth of the quinonoid at 508 nm can be described over most of its time course by the sum of two first-order processes. However, data taken beyond 6 s revealed a third slower first-order growth. The relatively long time required to collect data during the third phase made it technically difficult to simultaneously study all three phases. Therefore, the results presented in Table II were obtained in the fixed-wavelength mode so that data for the fast phase could be more precisely determined. These biphasic data were analyzed with eq 2 to give the rate constants for each phase and the total absorbance change as well as the fraction of the absorbance change attributable to each phase. A dissociation constant ($K_D = 0.67 \pm 0.01$ mM) for the formation of quinonoid was determined by a weighted least-squares analysis, as suggested by Wilkinson (1961), of the reciprocal total ΔA at 508 nm as a function of the reciprocal ethionine concentration. This is in close agreement with the value of 0.52 mM for the overall process given by Watanabe & Snell (1977). A similar treatment of ΔA_1 gave $K_D = 0.50 \pm 0.04$ mM for the fast process. Note that under these conditions (pH etc.) ΔA_1 and ΔA_2 were roughly of equal amplitude. The values for k_1' also exhibited a hyperbolic dependence on ethionine concentration (treatment not shown) giving a dissociation constant of 2.6 ± 0.2 mM for the formation of the Michaelis complex (or Schiff base) between tryptophanase and ethionine and $k_1' = 20.6 \pm 0.6$ s⁻¹ at infinite ethionine concentration at pH 8.0.

The rate constant k_2' for the slow phase does not show a hyperbolic behavior with increasing ethionine concentrations but is essentially constant below 1.4 mM ethionine concentrations, suggesting that k_2' reflects an enzyme conformational change. When the interaction of alanine with tryptophanase was examined under comparable conditions (Table II), the value of k_1' was substantially smaller than those obtained with

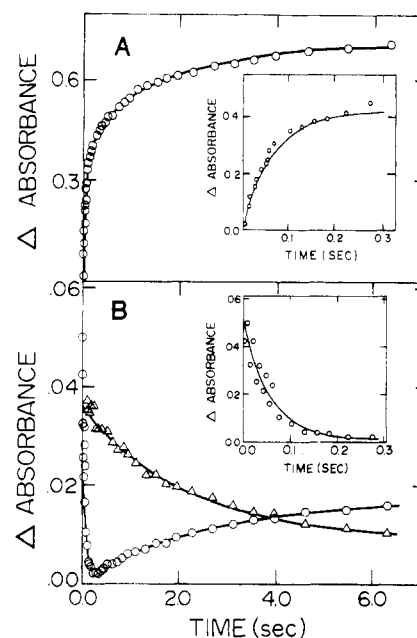


FIGURE 1: Changes in tryptophanase absorbance at 337 and 420 nm as a function of time after mixing with ethionine in 25 mM K-Hepps, pH 8.0, 0.2 M KCl, 1 mM EDTA, 10 μ M pyridoxal-P, and 0.2 mM DTT. After mixing, concentrations were 10 mM ethionine and 0.65 mg mL⁻¹ tryptophanase. (A) The overall absorbance changes at 508 nm. The data for the first 0.3 s are expanded in the inset. The line through the data in the inset was calculated by using eq 1 with the rate constant and amplitude for the fast phase, k_1' , given in Table I; the line through all data given in (A) was calculated with the rate constants and amplitudes for both phases. (B) (O) the overall absorbance changes at 420 nm; (Δ) the overall absorbance changes at 337 nm. The rapid decrease in absorbance at 420 nm is expanded in the inset. The lines were calculated by using eq 1 with the parameters listed in Table I.

ethionine, but the values obtained for k_2' were essentially the same as those obtained with ethionine. Since k_2' is comparable for both inhibitors the data support our previous suggestion that k_2' reflects an enzyme conformational change.

Effect of pH on Quinonoid Formation. Since the relative amounts of the 337- and 420-nm forms of tryptophanase depend on pH and since the 420-nm form appeared to be poised for reaction, we examined the rate and amplitude of quinonoid formation when tryptophanase was allowed to react with 5 mM

Table III: Rate Constants and Relative Amplitudes for Triphasic Growth of Quinonoid Formed from Tryptophanase and Ethionine at Three pH Values^a

pH	k_1' obsd (s ⁻¹)	k_1' calcd ^b (s ⁻¹)	k_2' (s ⁻¹)	k_3' (s ⁻¹)	% of total ΔA in each phase			
					(ΔA_1) obsd	(ΔA_1) calcd ^c	ΔA_2	ΔA_3
7.2	9.7 (2) ^d	7.2	0.82 (3)	0.132 (4)	70 (1)	89	20.0 (3)	9.7 (3)
7.2	9.9 (2)		0.87 (3)	0.166 (4)	69 (1)		19.8 (3)	11.0 (3)
8.0	15.5 (6)	12.3	0.75 (2)	0.109 (2)	49 (1)	55	35.2 (3)	16.2 (3)
8.0	16.2 (5)		0.79 (1)	0.114 (2)	49 (1)		35.1 (3)	16.2 (3)
8.7	17 (4)	20.3	0.70 (4)	0.090 (4)	30 (4)	23	43 (1)	27 (1)
8.7	23 (2)		0.74 (1)	0.093 (2)	29 (1)		48 (1)	23 (1)

^a The concentrations of reaction components after mixing were 25 mM K⁺-Hepps, pH_i, 0.1 M KCl, 0.5 mM EDTA, 0.05 mM pyridoxal-P, 0.1 mM DTT, 5 mM ethionine, and 0.78 mg mL⁻¹ tryptophanase. ^b Calculated with eq 4 by using the best-fit parameters given in Table IV.

^c Calculated with eq 5 by using the best-fit parameters given in Table IV. ^d Numbers in parentheses are the marginal standard deviation estimates for the last significant figure.

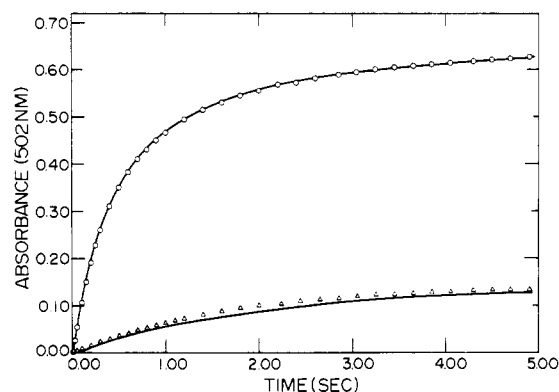


FIGURE 2: Effect of deuterium substitution at α position of alanine on rate and extent of quinonoid formation with tryptophanase. Tryptophanase was pushed against 0.45 M L-[α -¹H]alanine (O) and L-[α -²H]alanine (Δ) as described under Materials and Methods. The top line was calculated by using eq 2 with the values $\Delta A_1 = 0.43$, $\Delta A_2 = 0.22$, $k_1' = 2.4$ s⁻¹, and $k_2' = 0.38$ s⁻¹. The bottom line was calculated by using eq 1 with the values $\Delta A = 0.17$ and $k_1' = 0.49$ s⁻¹.

ethionine at pH 7.2, 8.0, and 8.7 as described under Materials and Methods. The data at each pH were collected for a period of 16.5 s and analyzed as the sum of three exponentials.³ The rate constants and relative amplitudes for all three phases are summarized in Table III. Examination of Table III reveals that as the pH is increased, k_1' also increases. In contrast k_2' and k_3' appear to be less sensitive to pH. The relative amplitude of the fast phase diminishes as the pH increases.

Deuterium Isotope Effect on Quinonoid Formation. Figure 2 shows that substitution of deuterium at the α position of the inhibitor, alanine, affects both the extent and rate of quinonoid formation. At equilibrium ~ 4.5 times more quinonoid is formed from L-[α -¹H]alanine than from L-[α -²H]alanine. The progress curve for quinonoid formation from L-[α -¹H]alanine was biphasic with $k_1' = 2.4 \pm 0.01$ s⁻¹ and $k_2' = 0.38 \pm 0.01$ s⁻¹. With deuterium at the α position, the two apparent first-order rate constants, k_1' and k_2' , were too close in value to be separated by our curve-fitting procedures. Therefore, the data were fit with a single exponential which gave $k_1' = 0.49 \pm 0.01$ s⁻¹ but with systematic deviations which suggested the presence of two exponentials with similar rate constants. It thus appears that the effect of deuterium substitution is to slow down the fast phase of quinonoid growth while leaving the slow phase virtually unchanged. This is interpreted as

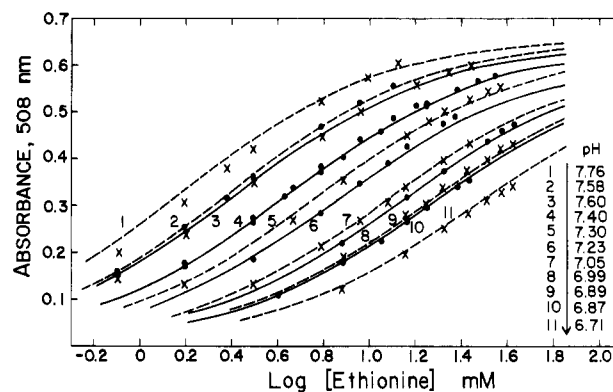
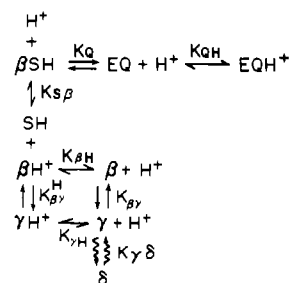


FIGURE 3: Effect of pH on equilibrium for reaction between L-ethionine and tryptophanase. Tryptophanase (18.5 mg mL⁻¹) was dialyzed extensively at 4 °C against 1 mM imidazole-HCl, pH 8.0 containing 0.2 M KCl, 0.1 mM pyridoxal-P, 1 mM EDTA, and 10 mM mercaptoethanol. An aliquot to give a total enzyme concentration of near 2.2 mg mL⁻¹ was added to 0.9 mL of 25 mM imidazole-HCl, pH_i, 0.2 M KCl, 0.1 mM pyridoxal-P, 1 mM EDTA, and 10 mM mercaptoethanol. An aliquot of 0.16 M ethionine in 0.2 M KCl, 0.1 mM pyridoxal-P, and 1 mM EDTA at pH_i was then added to the cuvette, and the absorbance was measured at 508 nm. The final pH of each titration was measured after addition of the last aliquot of ethionine. Titration curves at pH 7.10 and pH 7.20 (14 data pairs) were omitted from the figure. The lines were calculated by using eq 3 with the constants given in Table IV.

Scheme I



additional evidence that the slower phase reflects an enzyme conformation change.

pH Dependence of Equilibrium Reaction of L-Ethionine with Tryptophanase. The effect of pH on the equilibrium of the reaction between ethionine and tryptophanase is presented in Figure 3 as a series of titration curves obtained at various pH values. Each line of Figure 3 was calculated as described under Discussion. Note that the apparent K_D for ethionine decreases while ΔA_∞ , the calculated absorbance change at infinite ethionine, increases as the pH increases.

Discussion

The results presented in this paper, together with the results of the incremental pH-jump and pH-drop studies (June et al.,

³ It should be noted that the extraction of rate constants and amplitudes for three simultaneous exponential processes is numerically a difficult problem with strong coupling among the parameters. On the other hand, since the fit of these data over the entire time range to only two exponentials was very poor, it was necessary to analyze the data in terms of three exponentials.

Table IV: Best-Fit Parameters of Equations 3 and 4 Based on Scheme I for Data from Figure 4 and Table II and Their Marginal Standard Deviation Estimates

parameters	value	SD	
		value	%
$K_{S\beta}$	6.9×10^5	0.5×10^5	7
K_Q	$1.23 \times 10^{-7} \text{ M}$	0.09×10^{-7}	7
K_{QH}	$3.3 \times 10^{-8} \text{ M}$	0.3×10^{-8}	8
k_Q	25.7 s^{-1}	1.5	6
$\epsilon_{508\text{nm}}$	$40\,400 \text{ M}^{-1} \text{ cm}^{-1}$	500	1.2

1981) are in agreement with the stoichiometry of the model presented in Scheme I. Evidence for that portion of Scheme I involving the three slowly interconvertible enzyme conformation manifolds, β , γ , δ , was given in the preceding paper (June et al., 1981). The addition to this new scheme provides for the interaction of a competitive inhibitor, ethionine (SH^+), to form a quinonoid (EQ and EQH) absorbing at 508 nm.

Several lines of evidence support the argument that conformation β interacts directly with the inhibitors as portrayed in Scheme I. First, the rate of disappearance of the 420-nm absorbance is the same within experimental error as that of the fast phase of quinonoid formation at 508 nm (Table I). Second, the rate of disappearance of the 337-nm absorbance, designated by k_2' , is the same as the rate of the slow phase of quinonoid formation and is essentially unaffected by inhibitor concentration or the nature of the inhibitor (Table II). Third, the average values for k_2' of $0.51 \pm 0.14 \text{ s}^{-1}$ and $0.47 \pm 0.15 \text{ s}^{-1}$ obtained with ethionine and alanine, respectively (Table II), agree closely with the rate constant for the conversion of conformation γ to conformation β following a rapid decrease in pH (June et al., 1981). Thus, it appears that the 337-nm form of tryptophanase (γ conformation) does not form quinonoid directly but is first converted to the β conformation, the active form of the enzyme, which forms a Schiff base from which the α proton is removed.

That conformation β interacts with the inhibitor to form quinonoid is also supported by a comparison of the pH dependence of the relative amplitudes of the fast and slow phases of quinonoid growth with the amounts of enzyme in the β and γ conformations at equilibrium. As predicted by the equilibrium distribution of the various conformational forms as a function of pH [see Table I of June et al. (1981)], the percentage of the total quinonoid growth that occurs in the fast phase (ΔA_1) is largest at pH 7.2 where the β conformation predominates and becomes progressively smaller as the pH is increased (Table III). The percentages are as follows: at pH 7.2, $\beta + \beta\text{H}^+ = 86\%$, $\Delta A_1 = 70\%$; at pH 8.0, $(\beta + \beta\text{H}^+) = 55\%$, $\Delta A_1 = 49\%$; at pH 8.7, $(\beta + \beta\text{H}) = 22\%$, $\Delta A_1 = 29.5\%$. One would not expect exact agreement between the calculated and observed values because the calculated percentage distribution of the enzyme forms given in Table II of June et al. (1981) includes only the β and γ manifolds while the total absorbance change used to calculate the percentage ΔA_1 given in Table III includes all forms of the enzyme which can ultimately form the quinonoid.

The kinetics of quinonoid formation, the amplitudes of the slow and fast phases, and the pH dependence of the rate of interconversion of the various forms of tryptophanase are thus consistent with the model presented in Scheme I. The question which remains is whether the model is also compatible with equilibrium data for the formation of the quinonoid. An attempt to fit the data to a model which did not include the protonation of EQ gave a "best-fit" value of $K_{S\beta}$ which differed from that required to fit the rate data by 1 order of magnitude.

Scheme I (which is not claimed to be unique) was found to be compatible with both the rate and the equilibrium data. For evaluation of the new equilibrium constants $K_{S\beta}$, K_Q , and K_{QH} and the rate constant k_Q , the pH-dependent equilibrium data shown in Figure 3 and the fast rate constant k_1' (Table II) as a function of ethionine concentration were *simultaneously* fit to eq 3 and 4 with KINFIT4 (Dye & Nicely, 1971).

$$\Delta A = \Delta A_{\max}(1 + [\text{H}^+]/K_{QH}) / \left[1 + [\text{H}^+] \left(\frac{1}{K_{QH}} + \frac{1}{K_Q} + \frac{K_{\beta\text{H}}K_{S\beta}}{K_Q[\text{SH}^+](1 + K_{\beta\gamma})} \right) + \frac{[\text{H}^+]^2 K_{S\beta}}{K_Q[\text{SH}^+](1 + K_{\beta\gamma}\text{H})} \right] \quad (3)$$

$$k_1' = \frac{k_Q}{1 + \frac{K_{S\beta}}{[\text{SH}^+]([\text{H}^+] + K_{\beta\text{H}})}} + \frac{k_Q[\text{H}^+]}{K_Q \left(1 + \frac{[\text{H}^+]}{K_{QH}} \right)} \quad (4)$$

These equations follow directly from Scheme I and utilize the values of equilibrium constants $K_{\beta\gamma}$, $K_{\beta\text{H}}$, and $K_{\beta\gamma}\text{H}$ which were previously determined (June et al., 1981) together with the new parameters $K_{S\beta}$, K_Q , K_{QH} , and k_Q . The additional parameter, ΔA_{\max} , given in eq 3 is the maximum change in absorbance at 508 nm at an infinite concentration of SH^+ and at $[\text{H}^+] = 0$. It should be noted that eq 3 predicts a linear variation of $1/\Delta A$ with $1/[\text{SH}^+]$ at a fixed pH. Thus, a more conventional data treatment might evaluate an effective binding constant and maximum value of ΔA at *each* pH, followed by an examination of the pH dependence of these parameters. The present method of treating the data handles all 103 data pairs of the equilibrium data of Figure 3, together with the eight data pairs for k_1' given in Table II to produce the smallest set of residues, $(\Delta A_{\text{calcd}} - \Delta A_{\text{obsd}})$ and $[k_1'_{\text{calcd}} - k_1'_{\text{obsd}}]$. All input data were accompanied by appropriate error estimates so that a weighted least-squares fit could be obtained. The values of $K_{\beta\text{H}} = 2.0 \times 10^{-10} \text{ M}$, $K_{\beta\gamma} = 39$, and $K_{\beta\gamma}\text{H} = 0.045 \text{ M}$ were taken from Table II of June et al. (1981). The best-fit values of $K_{S\beta}$, K_Q , K_{QH} , k_Q , and ϵ_{508} together with their estimated marginal standard deviations are given in Table IV.

The value $40\,400 \text{ M}^{-1} \text{ cm}^{-1}$ for ϵ_{508} of the quinonoid was obtained from eq 4 by numerical evaluation at zero $[\text{H}^+]$ and infinite ethionine. Another estimate of ϵ_{508} can be made by using the data shown in Figure 1 and Table I together with the values of ϵ_{420} for form β ($4600 \text{ M}^{-1} \text{ cm}^{-1}$) and ϵ_{337} for form γ ($3500 \text{ M}^{-1} \text{ cm}^{-1}$) obtained from the pH-jump-drop experiments (June et al., 1981). By use of the values for $\Delta A_{508} = 0.747$ (Table I), $\Delta A_{420} = 0.049$ (Figure 1), and $\Delta A_{337} = 0.026$ (Figure 1), this gives $\epsilon_{508} = \Delta A_{508}/(\Delta A_{420}/\epsilon_{420} + \Delta A_{337}/\epsilon_{337}) = 41\,300 \text{ M}^{-1} \text{ cm}^{-1}$. These values for ϵ_{508} for quinonoid agree well with $\epsilon = 40\,000 \text{ M}^{-1} \text{ cm}^{-1}$ at 500 nm for a quinonoid obtained with serine transhydroxymethylase by Ulevitch & Kallen (1977) and an estimated value of at least 40 000 for the product of the reaction of amino acid esters with *N*-methylpyridoxal in ethanol (Schirch & Slotter, 1966).

The lines drawn through the experimental data in Figure 3 were calculated with eq 3 while k' values predicted by eq 4 are given in Tables II and III. The values for $(\Delta A_1)_{\text{calcd}}$ given in Table III were calculated with eq 5 by using the best-fit parameters given in Table IV.

The values for $(\Delta A_1)_{\text{calcd}}$ used to calculate $(\Delta A_1)_{\text{obsd}}/(\Delta A_1)_{\text{calcd}}$ given in Table II were obtained with eq 5 by using the best-fit parameters of Table IV. The value of $(\Delta A_1)_{\max}$ was calculated from the amount of enzyme in the β manifold

$$\Delta A_1 = \frac{(\Delta A_1)_{\max}(1 + [H^+]/K_{QH})}{1 + [H^+]\left(\frac{1}{K_{QH}} + \frac{1}{K_Q} + \frac{K_{\beta H}K_{S\beta}}{K_Q[SH^+]}\right) + \frac{[H^+]^2 K_{S\beta}}{K_Q[SH^+]}} \quad (5)$$

at pH 8.0 (55%) [see Table I of June et al. (1981)] and the value of ϵ_{508} for the quinonoid. This gives $(\Delta A_1)_{\max} = 0.486$ after accounting for the path length and adjusting to a specific activity of $51 \mu\text{mol min}^{-1} \text{mg}^{-1}$ by multiplying by 51/55. These calculated values of the amplitude of quinonoid growth during the fast phase are uniformly too large because we do not account for the fraction of enzyme present as forms α and δ and also because, in these fixed wavelength experiments, the monochromator was not set precisely at the absorbance maximum. Thus, although the ratios given in Table II are less than unity, the constancy of $(\Delta A_1)_{\text{obsd}}/(\Delta A_1)_{\text{calcd}}$ throughout the ethionine concentration range supports the proposed scheme.

Substitution of deuterium at the α position of alanine causes a dramatic decrease in both the extent of quinonoid formation and the rate of the fast phase of biphasic quinonoid growth. These results (Figure 2) show that the rate-limiting step for quinonoid formation is the abstraction of the α proton dictated by k_Q . Since the equilibrium constant of quinonoid formation is similarly affected and the yield of quinonoid remains low in the protic solvent water even after 5 s, the exchange of the abstracted α proton with solvent must be much slower than the reverse reaction. This predicted slow exchange of the abstracted α proton with solvent is supported by the observations of Vederas et al. (1978) which showed significant intramolecular transfer of the α proton of tryptophan to C-3 of indole during the tryptophanase catalyzed degradation of tryptophan.

Summary

Scheme I satisfactorily accounts for the following experimental observations with monovalent cation activated tryptophanase: (a) the rates and magnitudes of the 420–337-nm spectral interconversion of the holoenzyme as a function of pH (June et al., 1981); (b) the rate of biphasic quinonoid growth with the inhibitor ethionine and its relationship to the disappearance of the 337- and 420-nm forms of the enzyme (Figure 1); (c) the variation with pH and ethionine concentration of the rate constant for the fast phase of quinonoid growth (Tables II and III); (d) the variation in the relative and absolute amplitudes of the fast phase of quinonoid growth with pH and ethionine concentration (Tables II and III); (e) the variation of the equilibrium amplitude of quinonoid growth with pH and ethionine concentration (Figure 3); (f) the identification of the rate-determining steps in quinonoid formation as the abstraction of the α proton (fast phase) and the interconversion of enzyme forms β and γ (slow phase).

The only observation which is not in accord with Scheme I is the increase in the slow phase rate constant k_2' with ethionine concentration (Table II). The scheme predicts a decrease from a value of 0.43 s^{-1} at low ethionine concentrations to 0.24 s^{-1} at high concentrations. The observed increase from 0.4 s^{-1} at low ethionine concentrations to 0.7 s^{-1} at high concentrations suggests that either excess ethionine catalyzes the $\gamma \rightleftharpoons \beta$ conversion or that conformation γ can also form a Schiff base directly with ethionine at high concentrations which can then form the quinonoid.

Rate studies with amino acid substrates (to be published) are also in accord with the predictions of Scheme I. The extent of formation of the "active" β and γ manifolds from an "inactive" α manifold depends strongly on the nature of the activating monovalent cation and is also under investigation.

Acknowledgments

We acknowledge the assistance of Linda Siemsen during the analysis of some of the data and Dr. A. El Bayoumi for constructive criticism and discussion.

References

- Coolen, R. B., Papadakis, N., Avery, J., Enke, C. G., & Dye, J. L. (1975) *Anal. Chem.* **47**, 1649–1655.
- Dye, J. L., & Nicely, V. A. (1971) *J. Chem. Educ.* **48**, 443–448.
- Hogberg-Raibaud, A., Raibaud, O., & Goldberg, M. E. (1975) *J. Biol. Chem.* **250**, 3352–3358.
- June, D. S., Kennedy, B., Pierce, T. H., Elias, S. V., Halaka, F., Behbahani-Nejad, I., El-Bayoumi, A., Suelter, C. H., & Dye, J. L. (1979) *J. Am. Chem. Soc.* **101**, 2218–2219.
- June, D. S., Suelter, C. H., & Dye, J. L. (1981) *Biochemistry* (preceding paper in this issue).
- Morino, Y., & Snell, E. E. (1967) *J. Biol. Chem.* **242**, 2800–2809.
- Papadakis, N., Coolen, R. B., & Dye, J. L. (1975) *Anal. Chem.* **47**, 1644–1649.
- Schirch, L., & Slotter, R. A. (1966) *Biochemistry* **5**, 3175–3181.
- Suelter, C. H., & Snell, E. E. (1977) *J. Biol. Chem.* **252**, 1852–1857.
- Suelter, C. H., Coolen, R. B., Papadakis, N., & Dye, J. L. (1975) *Anal. Biochem.* **69**, 155–163.
- Suelter, C. H., Wang, J., & Snell, E. E. (1976) *FEBS Lett.* **66**, 230–232.
- Suelter, C. H., Wang, J., & Snell, E. E. (1977) *Anal. Biochem.* **76**, 221–232.
- Ulevitch, R. J., & Kallen, R. G. (1977) *Biochemistry* **16**, 5350–5354.
- Vederas, J. C., Schleicher, E., Tsai, M.-D., & Floss, H. G. (1978) *J. Biol. Chem.* **253**, 5350–5354.
- Watanabe, T., & Snell, E. E. (1977) *J. Biochem. (Tokyo)* **82**, 733–745.
- Wilkinson, G. N. (1961) *Biochem. J.* **80**, 324–332.